Supplementary Information (SI) for Reaction Chemistry & Engineering.

Supplementary information

Python Codes

Below is a link to the GitHub repository, where you can find the code and kinetic experiment results used to create the kinetic model. It will include both the kinetic fitting code and simulation code. Both developed codes are included in GitHub.

Note: Data for experimental results is in mol/L to align with the code's output

Colin Bailey developed all the code.

Methods

Kinetic Model Selection

Below will be two examples of other kinetic models that were attempted to be used for potential models.

Model 2:

The Arrhenius Parameter fitting code was the exact same as Model 1 (model included in main paper) except for no inclusion of Mono-Alkylated Ester (**7**) in the fitting process. No reversible reaction between DIPBA (**1**) and DIPBA Ester (**6**). So, this model was less complex than the model shared in the main paper.

Results:

Compound ID	**R^2**	**NRMSE**
4-HBA (**2**)	0.731	0.088
DIPBA (**1**)	0.643	0.134
Mono-Alkylated (**4**)	-1.519	0.338
4-HBA Ester (**5**)	-4.270	0.439
Sulfonated Impurity (**3**)	-12.613	0.803
DIPBA Ester (**6**)	-32.589	1.381

Table S1. Table of Fitting Values for Kinetic Model 2

Fittings for Arrhenius parameters were way worse than what was seen in the selected model. When Arrhenius parameters are implemented into the simulation code, you get the results below.

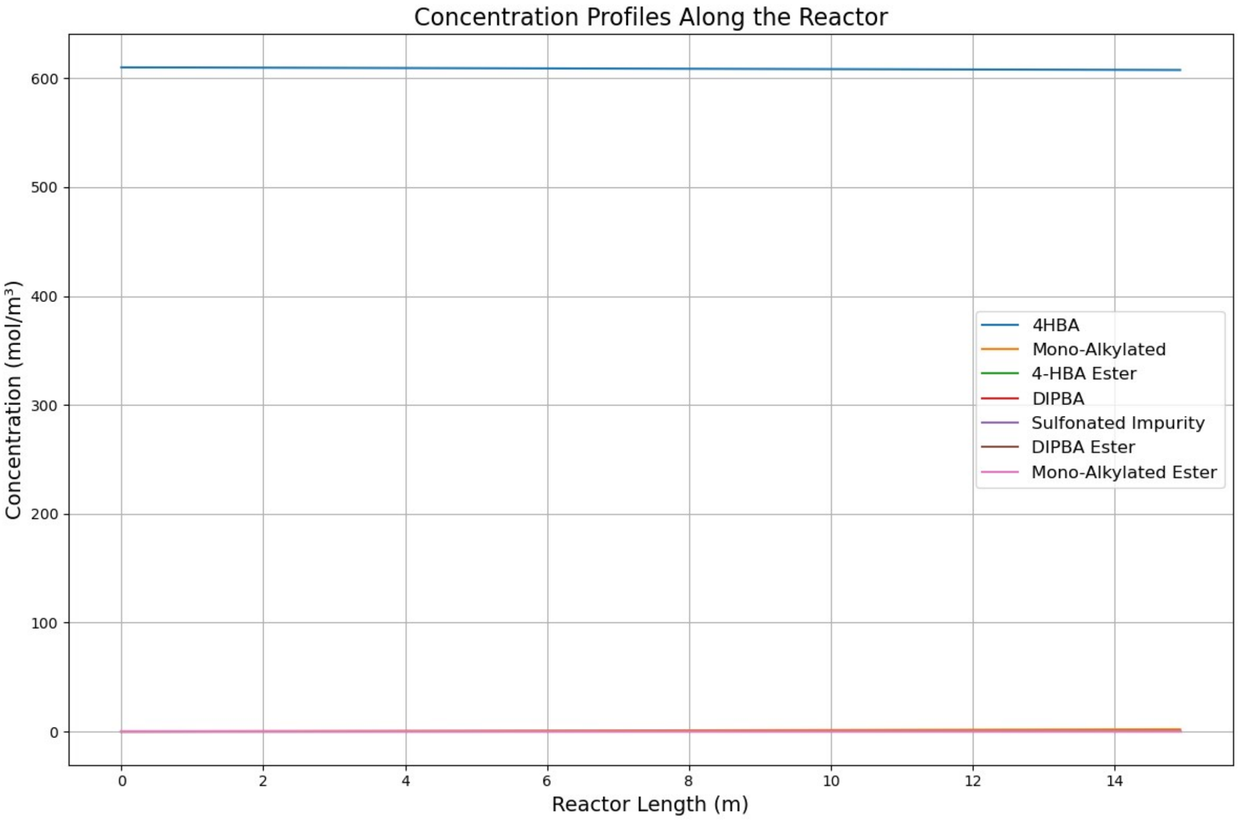

Figure S1. Figure of concentration along the reactor for Kinetic Model 2

Simulation shows almost no reaction because the value for the k_form that is found during this fitting is too small to allow the reaction to proceed.

Model 3:

The Arrhenius Parameter fitting code was the same as Model 1 (model included in main paper) except for a slightly different method to try and fit the k_form parameter for the formation of the carbocation. No reversible reaction between DIPBA (**1**) and DIPBA Ester (**6**). Results below:

Compound ID	**R^2**	**NRMSE**
4-HBA (**2**)	0.778	0.081
DIPBA (**1**)	0.718	0.120
Sulfonated Impurity (**3**)	0.667	0.127
Mono-Alkylated (**4**)	0.021	0.209
4-HBA Ester (**5**)	-0.167	0.210
DIPBA Ester (**6**)	-0.535	0.293

Table S2. Kinetic Model 3 R^2 fitting results

Arrhenius fitting values were better than what is seen in model 1 but when the found values are placed in the simulation code we get the results below.

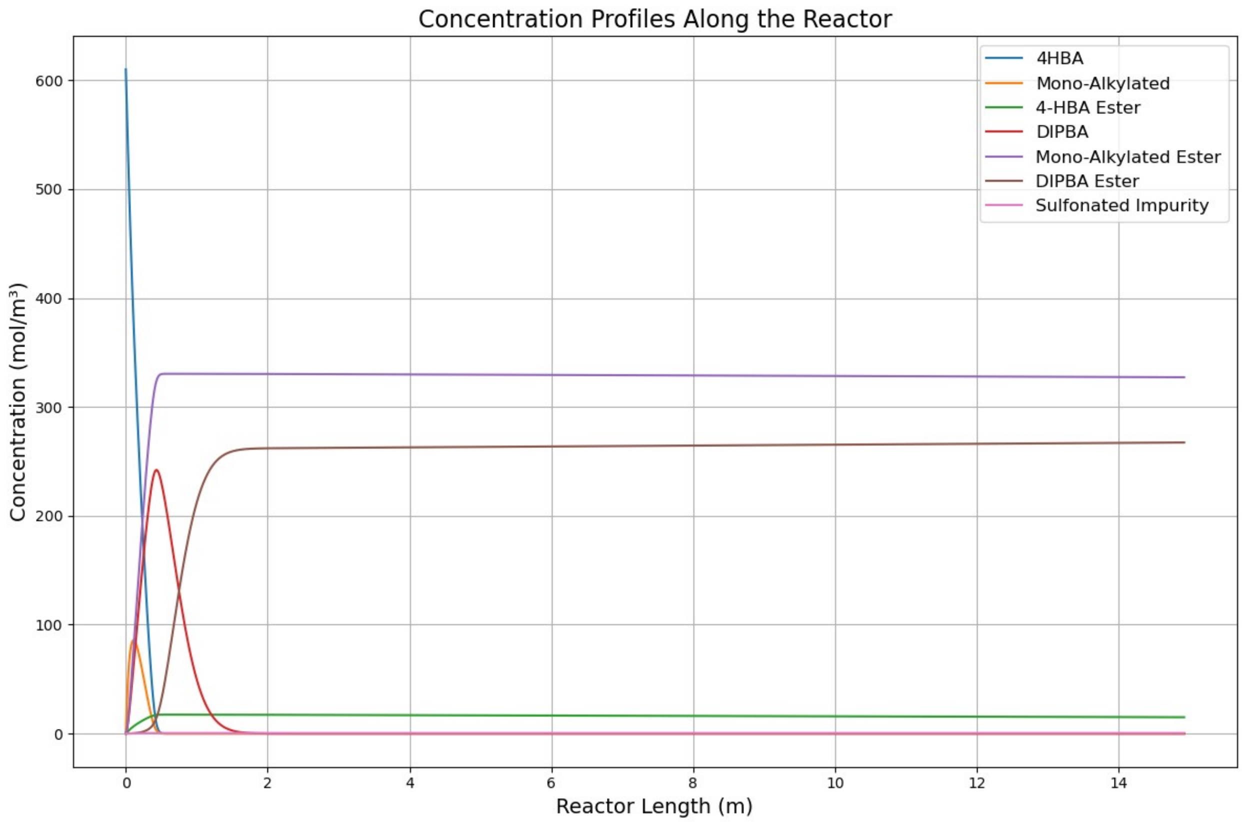

Figure S2. Figure of Simulated concentration profile along the reactor using the fitted Arrhenius parameters

When compared to Model 1, both alternative models showed notable limitations. Model 2, which excluded the mono-alkylated ester (**7**), produced significantly poorer overall fits and resulted in simulation outputs that showed minimal reaction progress along the reactor. Model 3 retained the mono-alkylated ester (**7**) but omitted the reversible reaction between DIPBA (**1**) and DIPBA Ester (**6**), while also modifying the approach used to calculate the carbocation formation rate (k_form). This combination led to an overestimation of both the mono-alkylated ester (**7**) and DIPBA Ester (**6**) concentrations, highlighting the importance of including both reversible steps and accurate intermediate representation for reliable simulation results.

Sample preparation:

Samples were prepared using a systematic dilution strategy based on the initial concentration of the starting material to ensure consistent HPLC quantification. Reactions starting at 1.8 M were diluted 100-fold, those at 0.9 M were diluted 50-fold, and those at 0.45 M were diluted 25-fold before analysis. All samples were diluted in Acetonitrile to avoid impurity formation during analysis. These dilution factors were also used to back-calculate the actual reaction concentrations from the HPLC results, allowing for an accurate comparison across experiments.

HPLC Method:

The HPLC method used to quantify all compounds in this study was developed and validated by the analytical team at Virginia Commonwealth University (VCU). Method parameters, including column type, mobile phase composition, flow rate, and detection wavelength, were optimized to achieve adequate resolution for all species of interest. Full method details are provided below to ensure reproducibility.

Conditions:

Column: Agilent Eclipse XDB-C18 (250 x 4.6 mm; 5 µm)

Mobile Phase A: 0.1% H_3PO_4 in water

Mobile Phase B: Acetonitrile

Injection volume: 1 µL

Column temp: 40°C

Flow rate: 2.0 mL/min

Detector wavelength(s): 210 nm, 275 nm, 440 nm

LC Gradient Table:

Time (min)	%A	%B
0	80	20
0.5	80	20
8	40	60
14	40	60
18	10	90
25	10	90

Post-run equilibration: 2 min

Sample preparation: Prepare samples at 1 mg/mL in acetonitrile.

Retention Times

Compound	Time (min)	Relative RF (mg/mL)	Relative RF (M)
Diisoproplbenzoic Acid (DIPBA)	7.650	1	1
4-Hydroxybenzoic Acid (4-HBA)	2.153	0.827	0.514
Monoalkylated sulfoate ester	3.909	0.720	0.843
Monoalkylated Benzoic Acid	5.473	0.885	0.718
4-isopropoxybenzoic acid	7.142	0.601	0.487
Isopropyl 4-hydroxybenzoate	7.347	0.569	0.461
Dialkylated esterified BA (EP Imp P)	15.565	0.842	1.002
2,4,6-Triisopropyl phenol	18.182	0.484	0.582
Step 1 Pseudodimer	22.52	0.826	0.901

Notes:

*

$$Relative\ RF = \frac{\left(Analyte\ 2\ Peak\ Area. \middle/ Analyte\ 2\ Conc.\right)}{\left(Analyte\ 1\ Peak\ Area \middle/ Analyte\ 1\ Conc.\right)}$$

$$Conc.Imp = \left(\frac{Peak\ Area\ Im}{RRF\ Imp}\right.$$

Reproducibility and repeatability was tested with the same 1.00 mg/mL standard of DIPBA (**1**) run three times on the HPLC at the same time. Results are shared in table S1 below.

Metric	Inj. 1	Inj. 2	Inj. 3	Mean	RSD (%)
Peak Area (mAU*s)	3421.116	3450.642	3484.714	3452.157	0.92
Peak Heaight (mAU)	849.372	859.084	865.565	858.007	0.95
Retention Time (min)	7.646	7.651	7.652	7.650	0.042

Table S3. HPLC analytical repeatability from standard injections (n = 3)

Reactor Process Flow Diagrams

Process flow diagrams of reactor systems 1 and 2 are provided below

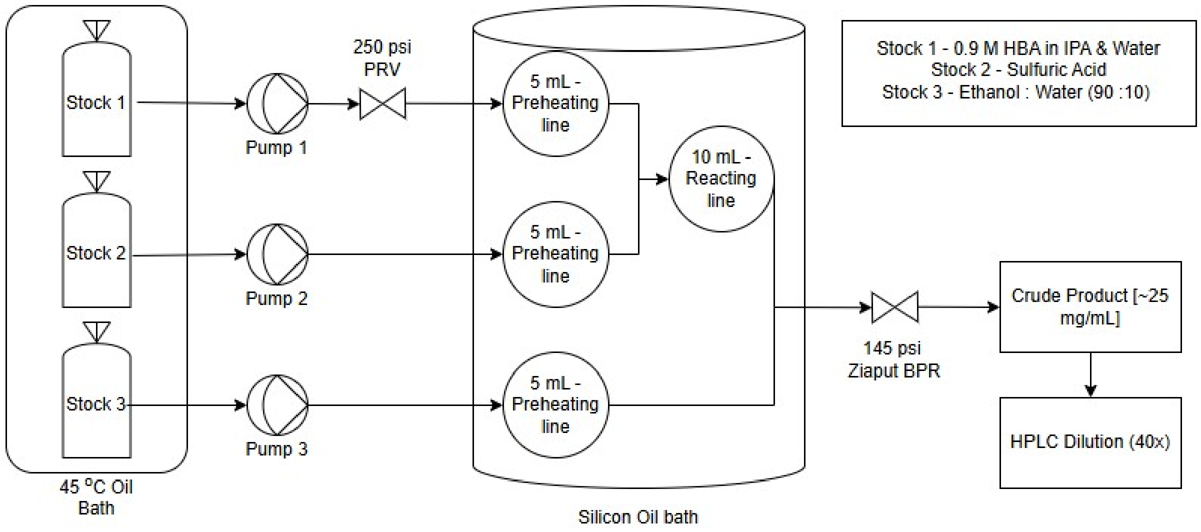

Figure S1. Kinetic Reactor System 1

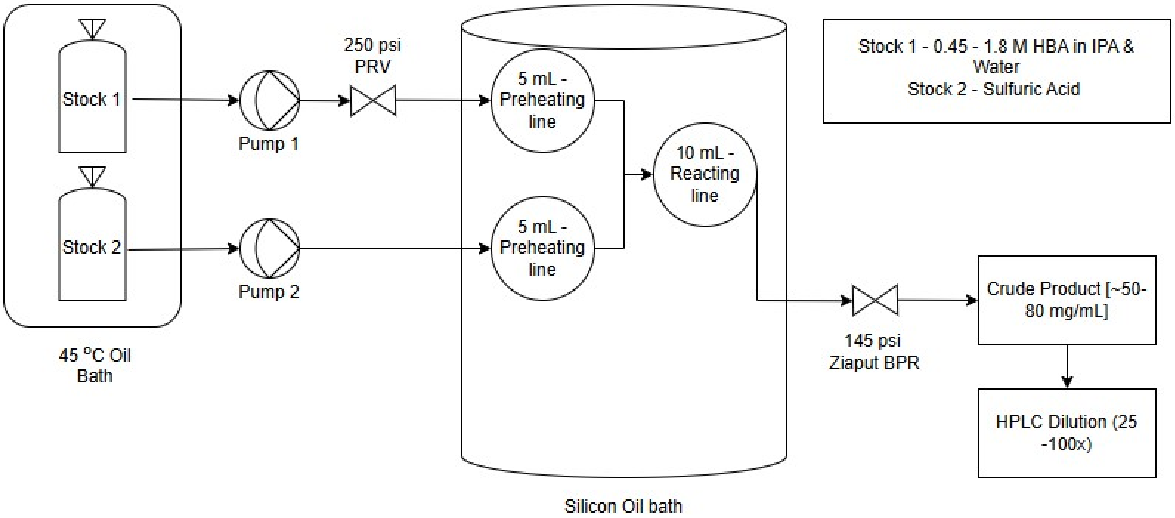

Figure S2. Kinetic Reactor system 2

Reactor System 1 Reproducibility Results

Below are the results from Reactor System 1, comparing performance between runs conducted with a dilution stream and those without. This comparison was performed using the same reactor configuration to evaluate the impact of dilution on solubility, conversion efficiency, and impurity formation under otherwise identical conditions. Some compounds included in the graph were not included in the kinetic study but are provided to show that none of them were affected by the addition of the dilution stream.

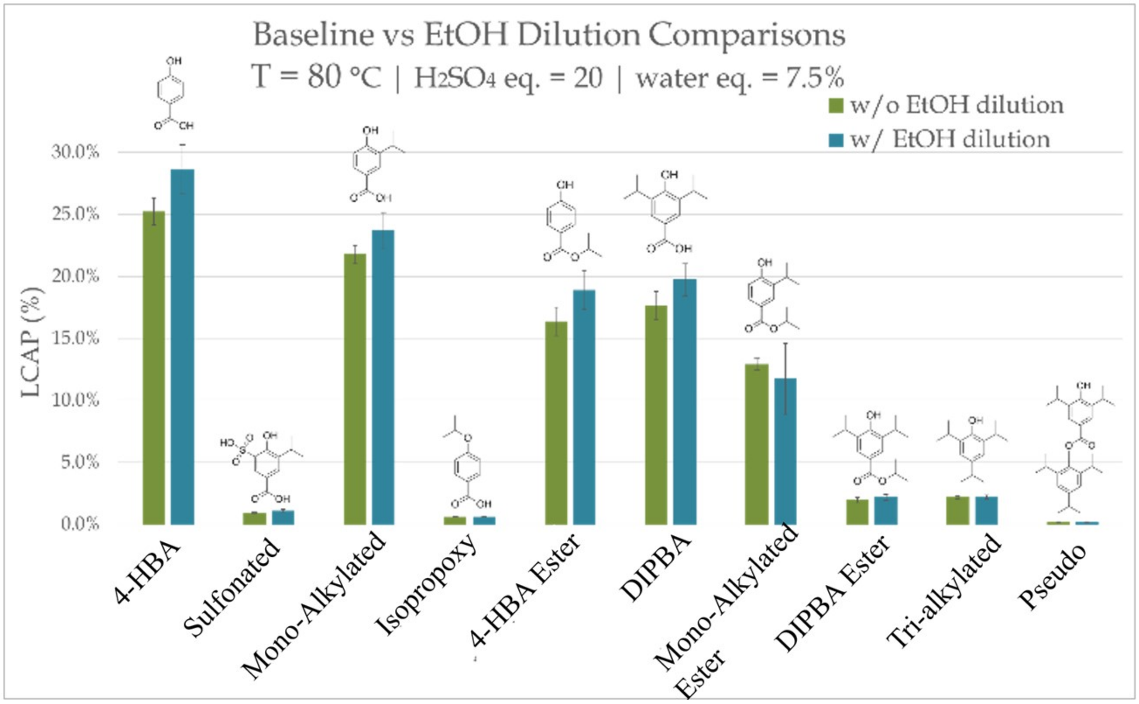

Figure S3. Results of Diluted vs baseline reaction conditions

Simulation results

Table S1 presents the simulated outlet concentrations for each species under various reaction conditions, using the fitted kinetic parameters. These results highlight trends in DIPBA formation and impurity profiles, supporting the model's predictive capability and its alignment with experimental observations.

Experiment Number	**Experiment Conditions**	HBA (**2**)	Sulfonated Impurity (**3**)	Mono-Alkylated (**4**)	4-HBA Ester (**5**)	DIPBA (**1**)	DIPBA Ester (**6**)
1	1.8 M 4-HBA, 80 °C, 15-minute residence time	0.0 %	6.78 %	0.0 %	0.0 %	71.6 %	21.6 %
2	1.8 M 4-HBA, 90 °C, 10-minute residence time	0.0 %	6.38 %	0.0 %	0.0 %	72.6 %	21.0 %
3	0.9 M 4-HBA, 80 °C, 15-minute residence time	0.0 %	6.12 %	0.0 %	0.0 %	63.8 %	30.1 %
4	0.9 M 4-HBA, 70 °C, 20-minute residence time	0.0 %	6.65 %	0.0 %	0.0 %	62.4 %	30.9 %
5	0.9 M 4-HBA, 84 °C, 17-minute residence time	0.0 %	5.96 %	0.0 %	0.0 %	65.6 %	28.4 %

Table S4. Results of all 5 simulations

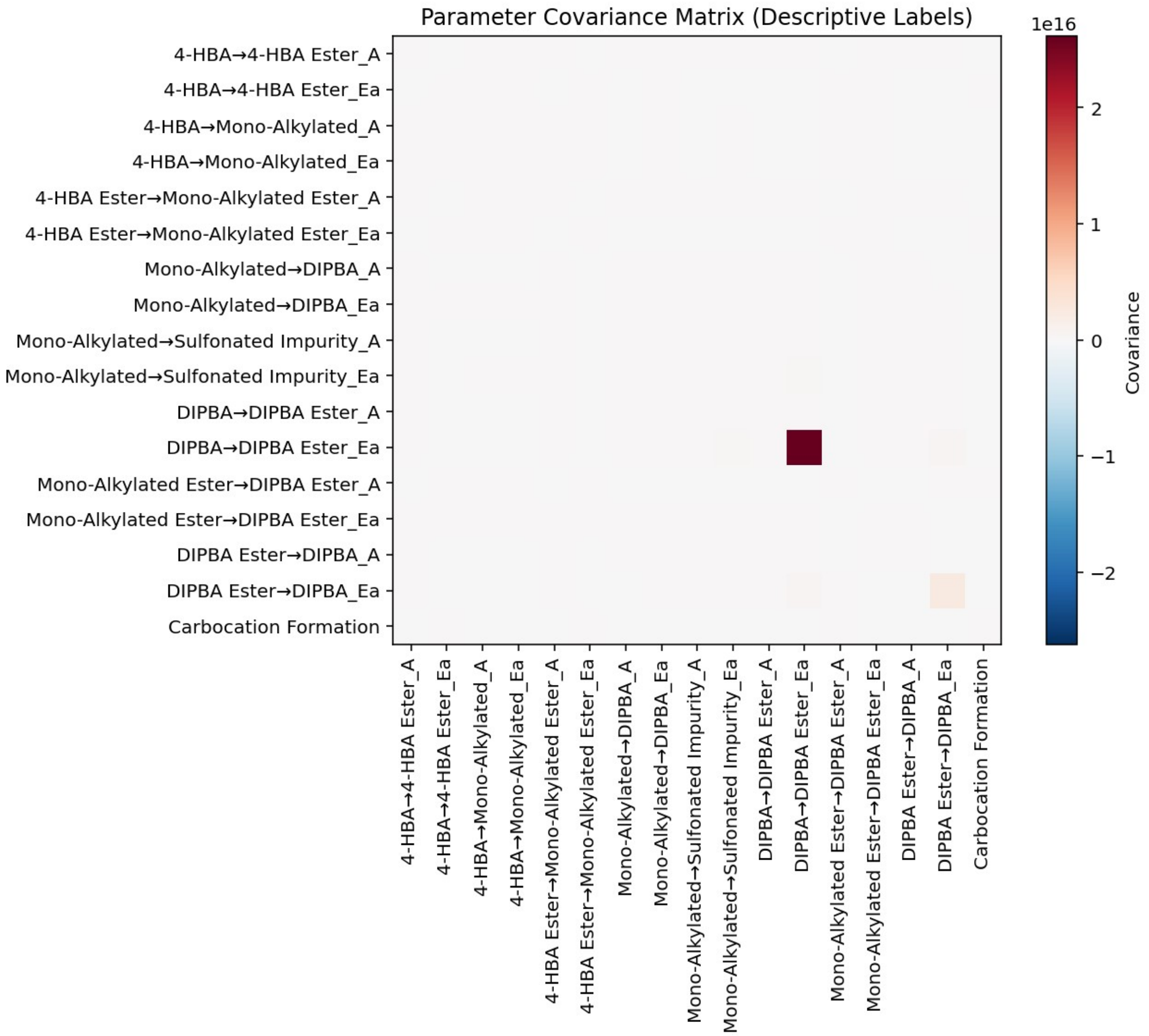

Figure S4*.* Covariance Heatmap

A covariance heatmap was generated to evaluate the degree of shared variability between the simulated and experimental species concentrations. Since covariance values are scale-dependent, the results primarily reflect differences in magnitude rather than underlying relationships. While the heatmap confirms consistency in variability between certain compounds, it does not provide additional mechanistic insight beyond the correlation analysis.

Figures of reaction profiles over time for experimental conditions and carbocation formation along the reactor.

Presented below are the outputs generated by the reactor simulation code, which detail the spatial concentration profiles of all key reaction species along the length of the reactor. In addition to tracking the evolution of each compound, the simulation also captures the formation and steady-state behavior of the carbocation intermediate, offering a comprehensive view of the reaction's progression under continuous flow conditions.

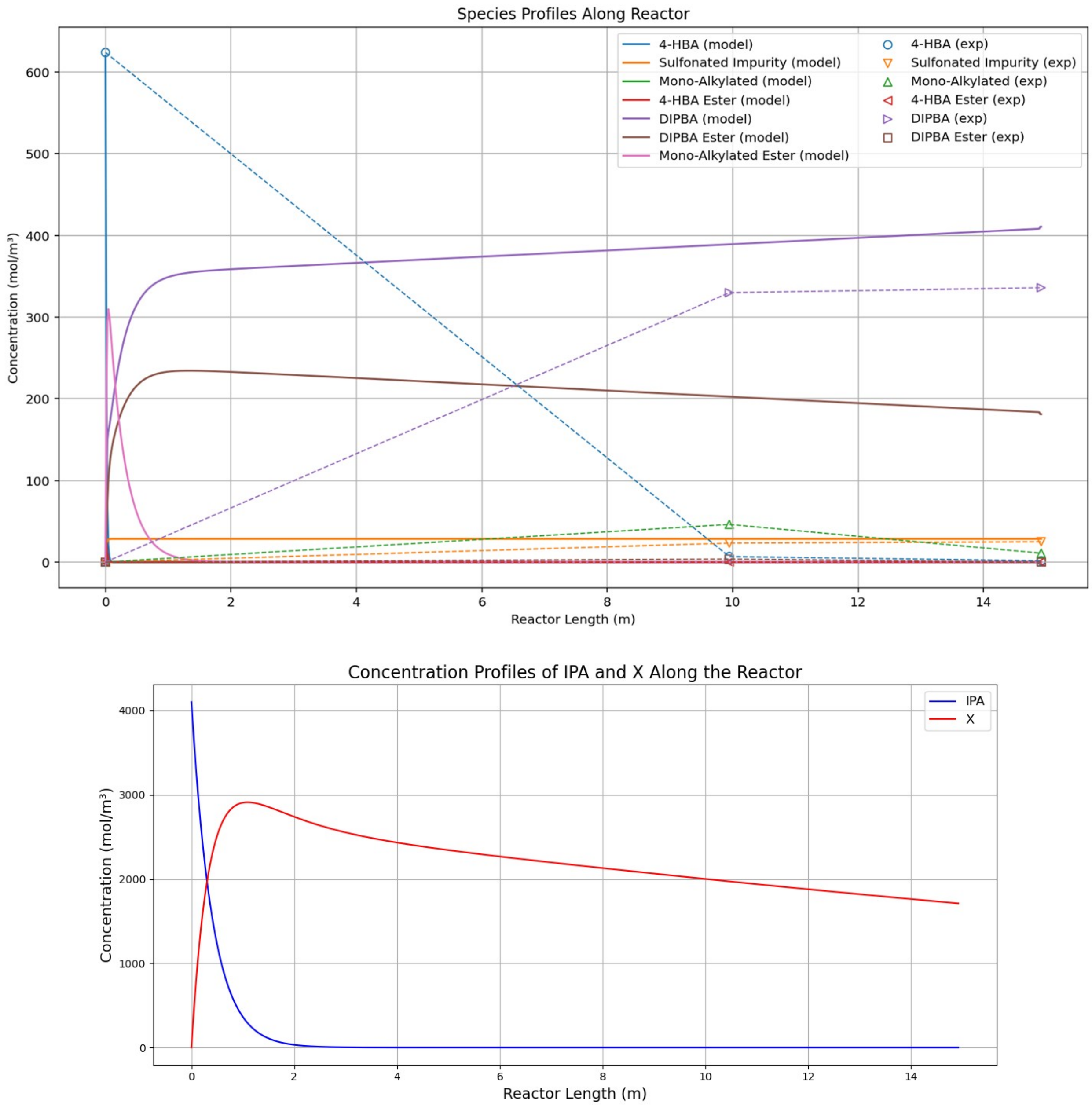

Figures S5. Experiment 1: Reaction conditions; 1.8 M 4-HBA (**2**), 80 °C, 15-minute residence time

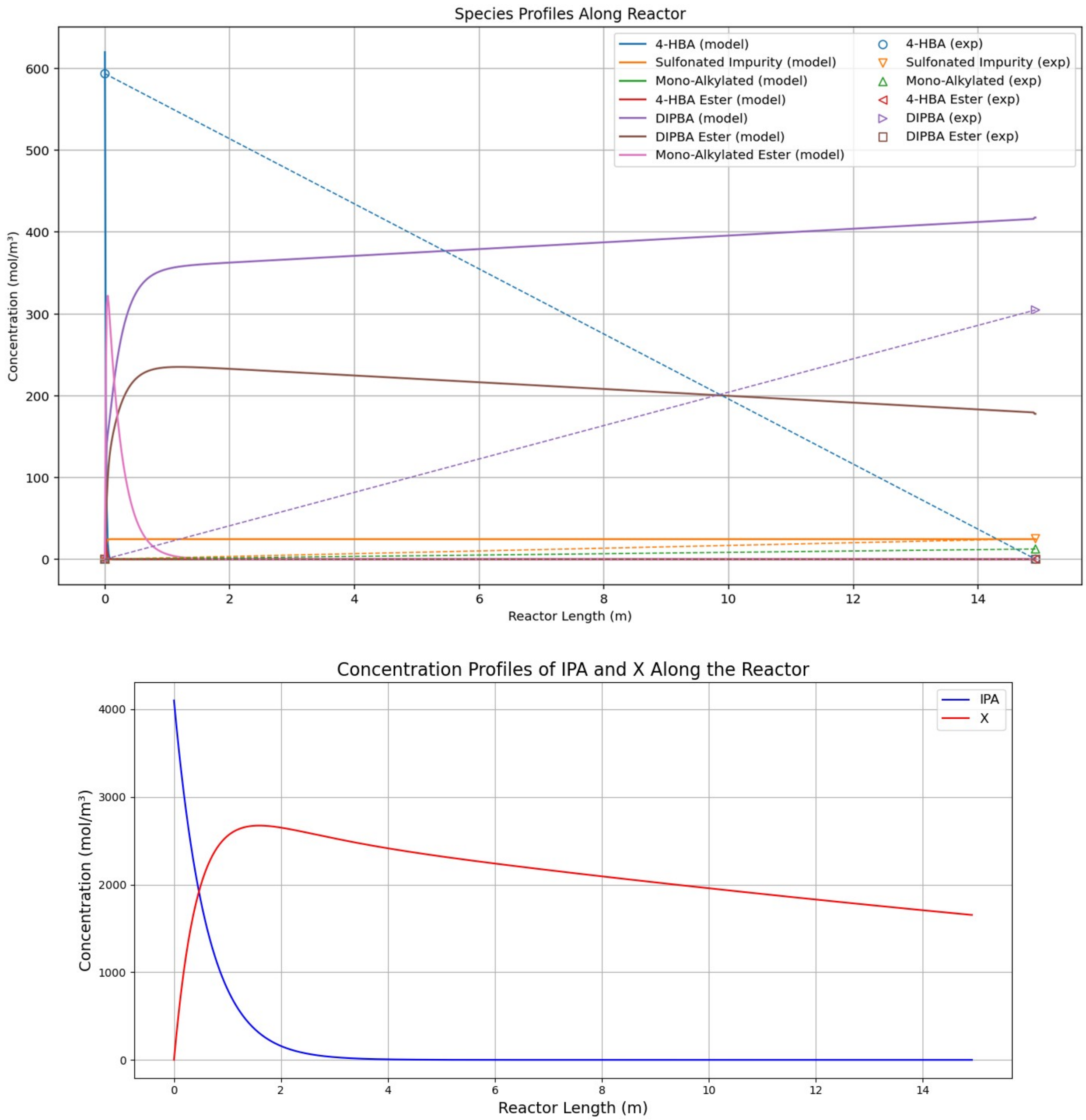

Figures S6. Experiment 2: Reaction conditions; 1.8 M 4-HBA (**2**), 90 °C, 10-minute residence time

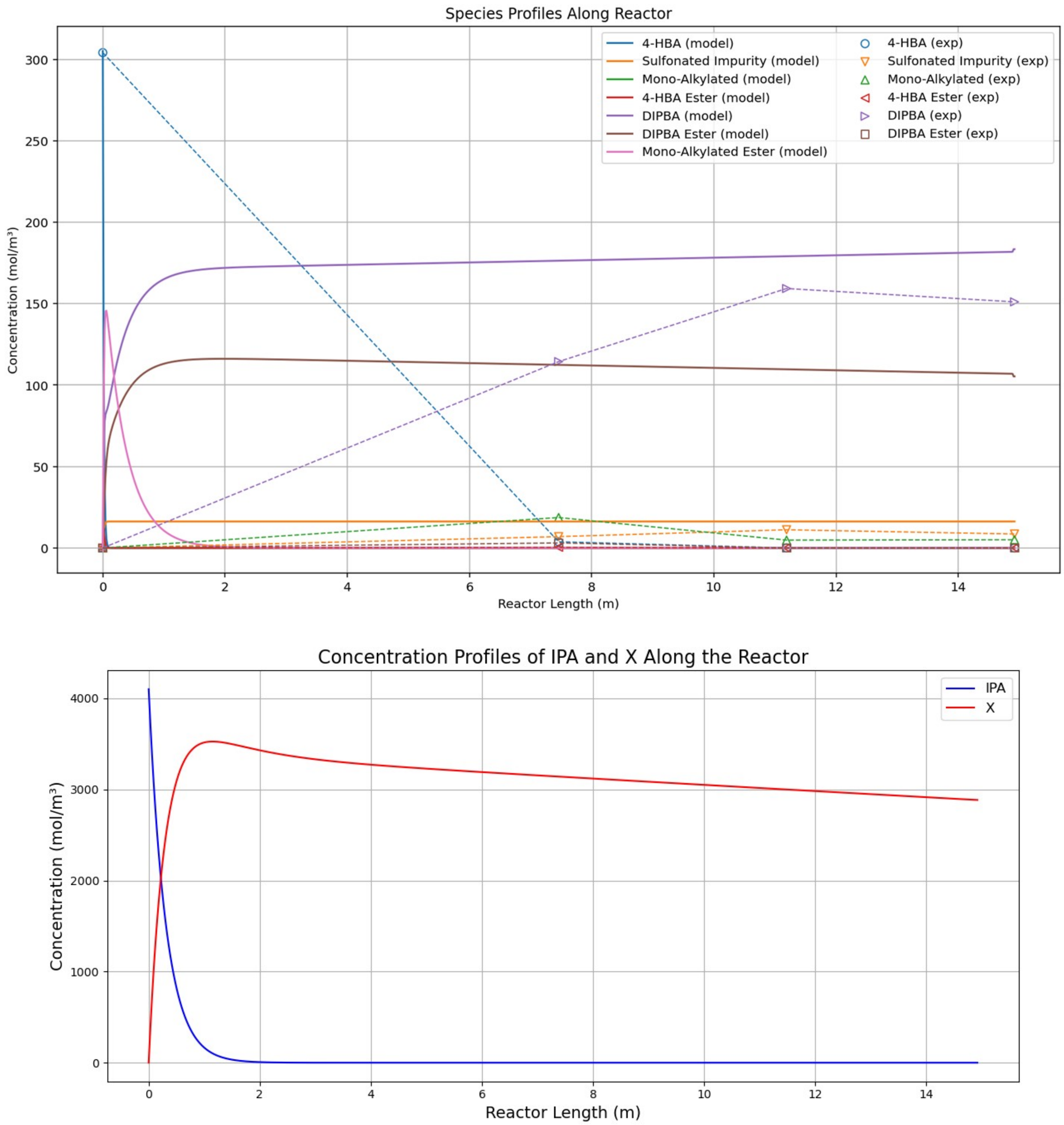

Figures S7. Experiment 4: Reaction conditions; 0.9 M 4-HBA (**2**), 70 °C, 20-minute residence time

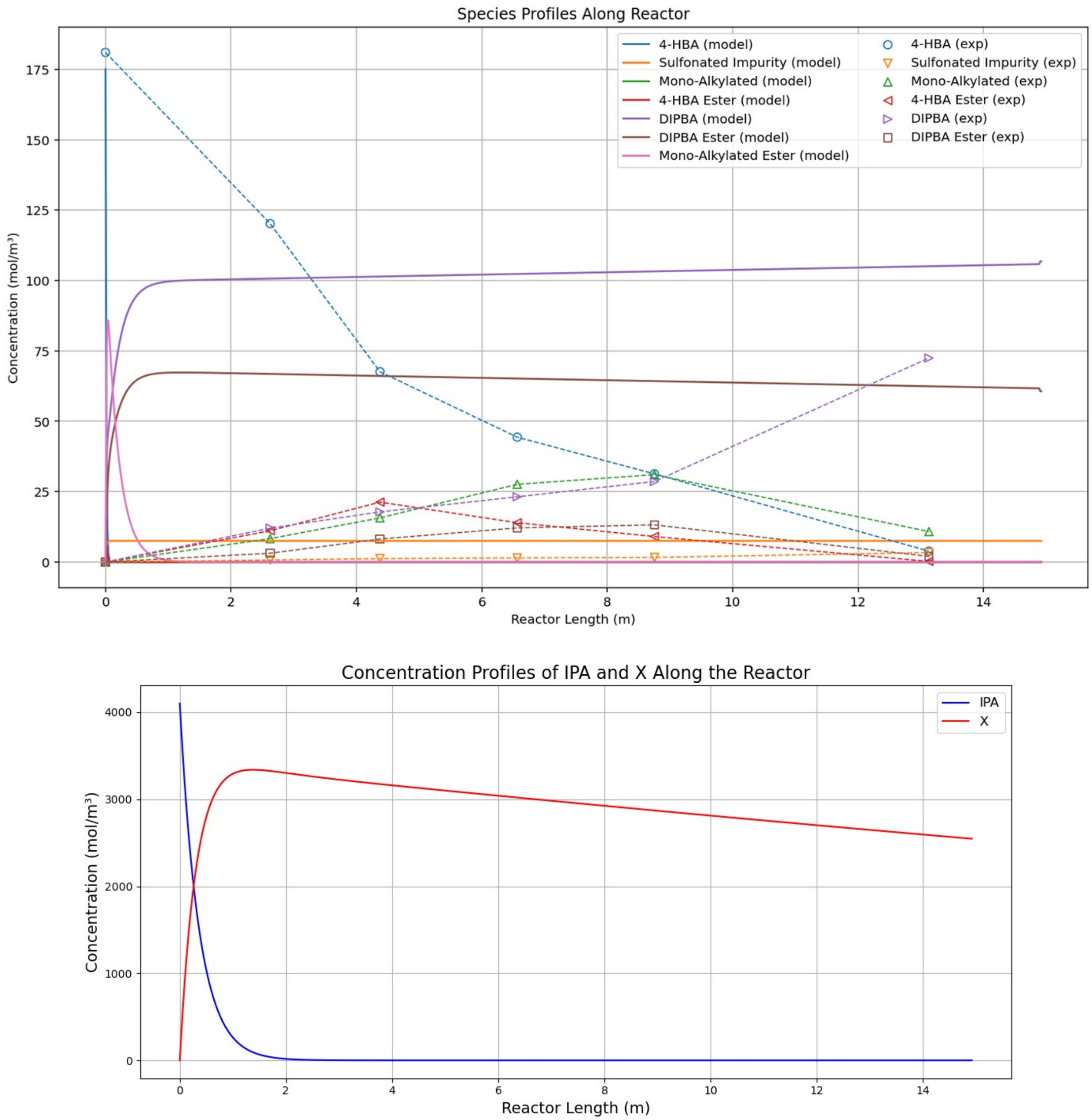

Figures S8. Experiment 5: Reaction conditions; 0.9 M 4-HBA (**2**), 84 °C, 17-minute residence time

Bar Graphs of Yields: Results of simulations vs experiments for all compounds

Below are graphs comparing the experimental yields with the corresponding simulated yields for each compound across all tested experimental conditions. These comparisons illustrate the model’s ability to capture reaction trends and highlight areas of agreement or deviation between predicted and observed outcomes.

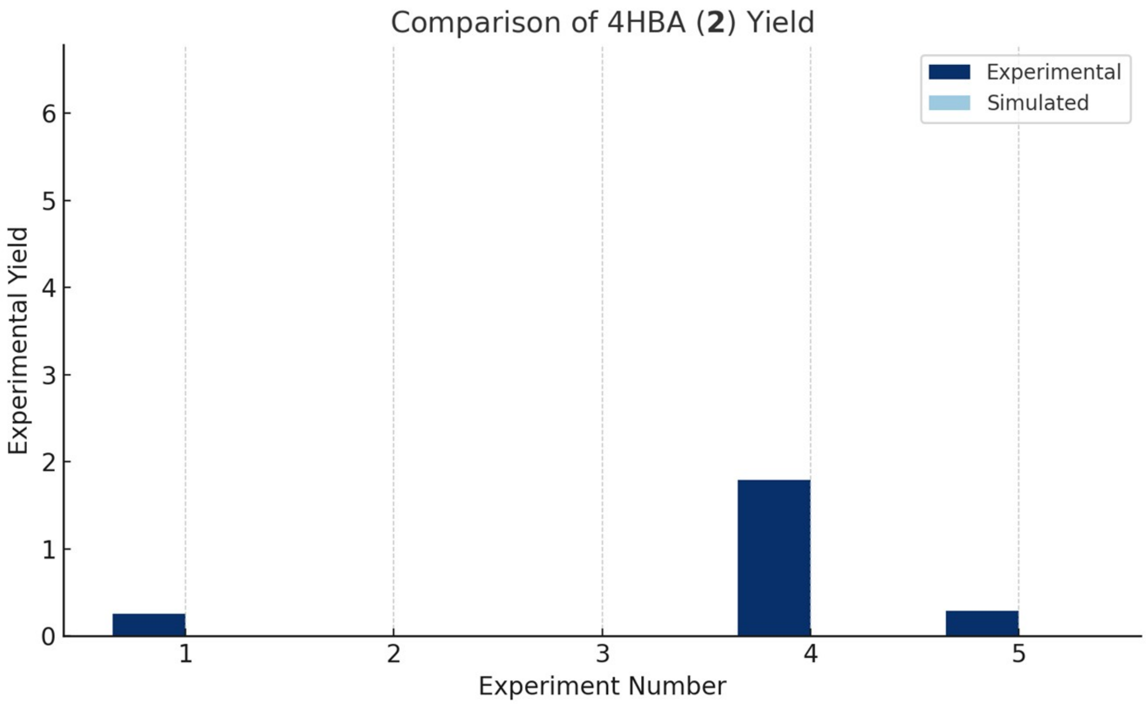

Figure S9. 4-HBA (**2**) Experimental vs Simulated Yield for all 5 experiments

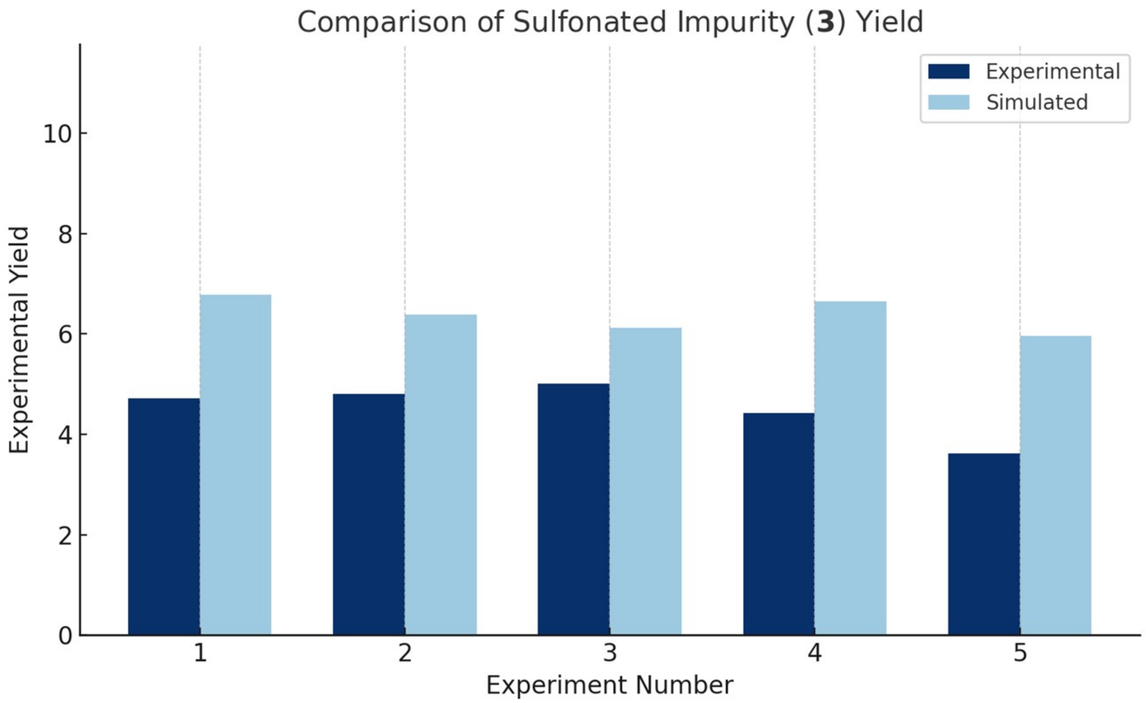

Figure S10. Sulfonated Impurity (**3**) Experimental vs Simulated Yield for all 5 experiments

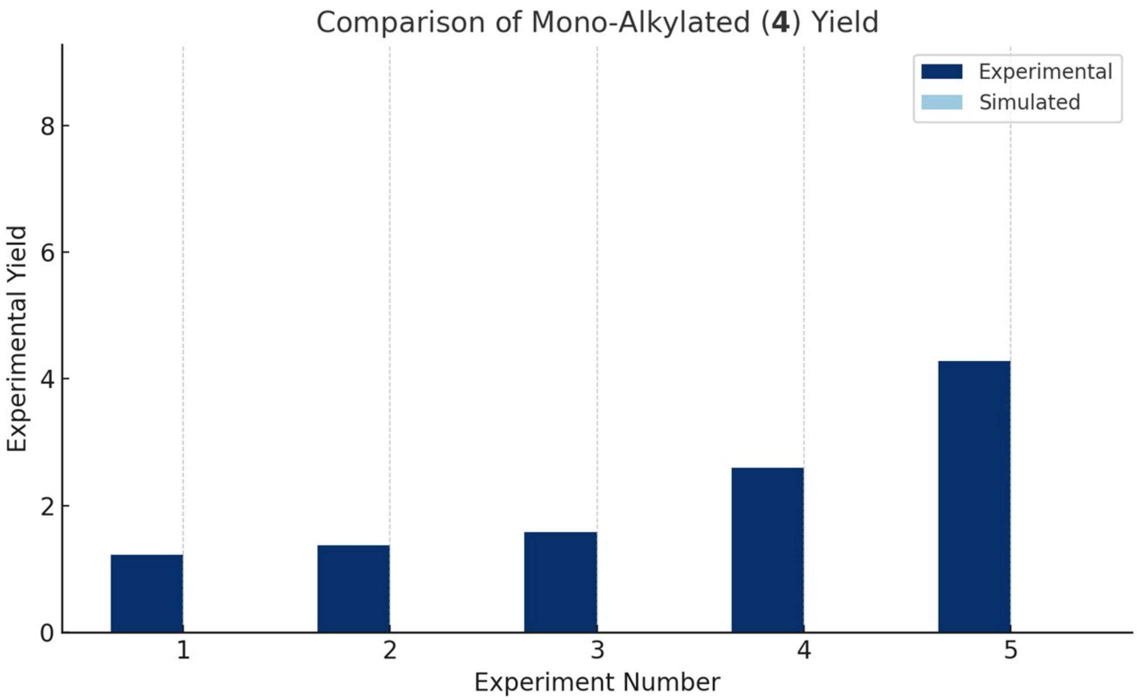

Figure S11. Mono-Alkylated (**4**) Experimental vs Simulated Yield for all 5 experiments

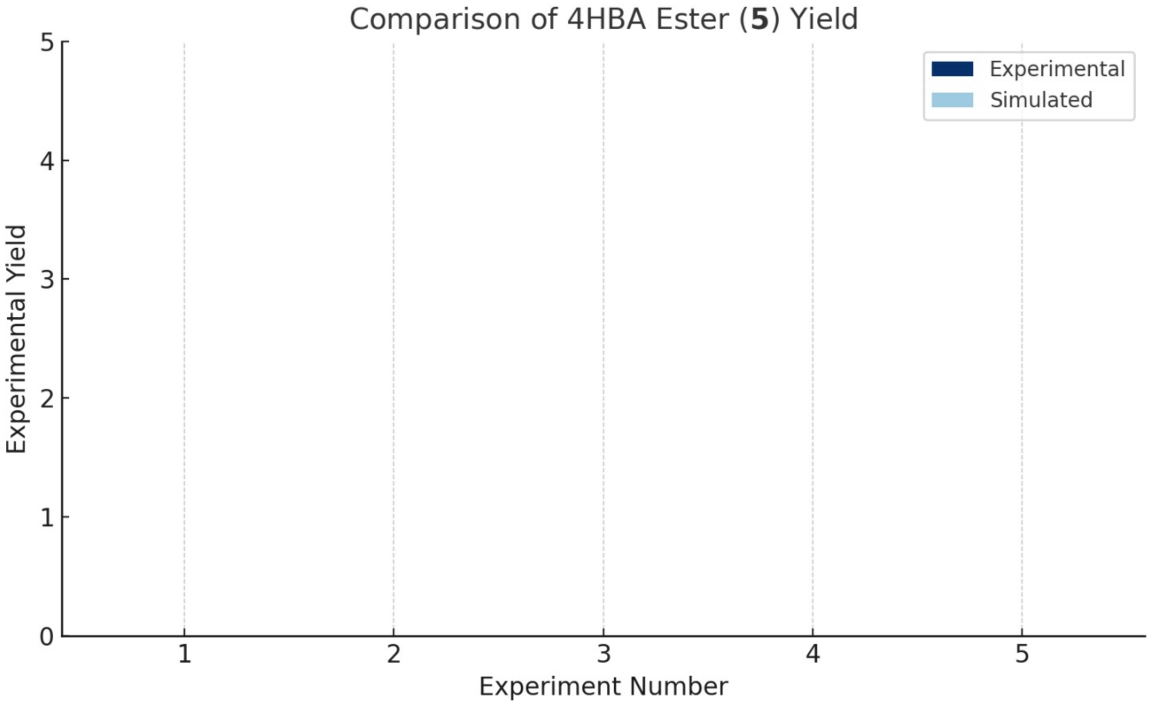

Figure S12. 4-HBA Ester (**5**) Experimental vs Simulated Yield for all 5 experiments

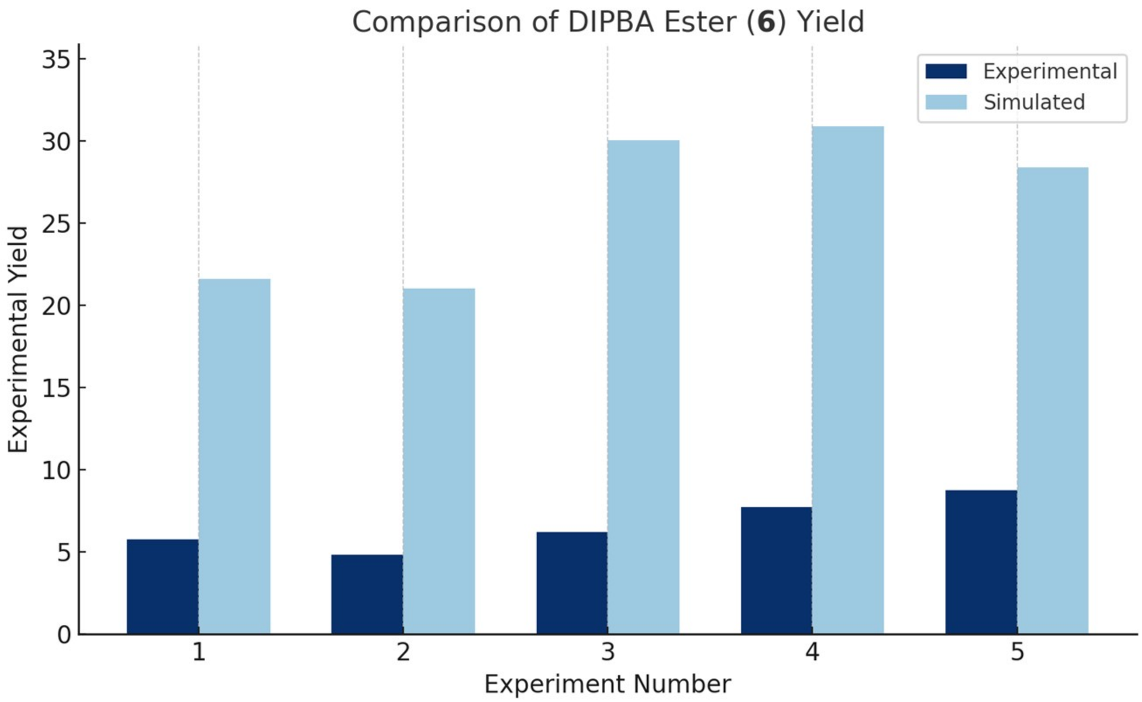

Figure S13. DIPBA Ester (**6**) Experimental vs Simulated Yield for all 5 experiments